PHYSICAL REVIEW D **79,** 054019 (2009)

Quarkonium states in an anisotropic QCD plasma

Adrian Dumitru,[1,2,3] Yun Guo,[4,5] Ágnes Mócsy,[6] and Michael Strickland[7]

[1]*Department of Natural Sciences, Baruch College, CUNY, 17 Lexington Ave, New York, New York 10010, USA*
[2]*RIKEN-BNL Research Center, Brookhaven National Lab, Upton, New York 11973, USA*
[3]*Graduate School and University Center, City University of New York, , 365 Fifth Avenue, New York, New York 10036, USA*
[4]*Helmholtz Research School, Goethe Universität, Max-von-Laue-Str. 1, D-60438 Frankfurt am Main, Germany*
[5]*Institute of Particle Physics, Huazhong Normal University, Wuhan 430079, China*
[6]*Department of Mathematics and Science, Pratt Institute, 200 Willoughby Avenue, Brooklyn, New York 11205, USA*
[7]*Department of Physics, Gettysburg College, Gettysburg, Pennsylvania 17325, USA*

(Received 19 January 2009; published 31 March 2009)

We consider quarkonium in a hot quantum chromodynamics (QCD) plasma which, due to expansion and nonzero viscosity, exhibits a local anisotropy in momentum space. At short distances the heavy-quark potential is known at tree level from the hard-thermal loop resummed gluon propagator in anisotropic perturbative QCD. The potential at long distances is modeled as a QCD string which is screened at the same scale as the Coulomb field. At asymptotic separation the potential energy is nonzero and inversely proportional to the temperature. We obtain numerical solutions of the three-dimensional Schrödinger equation for this potential. We find that quarkonium binding is stronger at nonvanishing viscosity and expansion rate, and that the anisotropy leads to polarization of the *P*-wave states.

DOI: 10.1103/PhysRevD.79.054019 PACS numbers: 12.39.−x, 11.10.St, 12.38.Mh, 12.39.Pn

INTRODUCTION

In the era of the relativistic heavy ion collider at Brookhaven and the large hadron collider at CERN the theoretical understanding of in-medium modifications of QCD bound states is expected to progress significantly. In this paper we focus on the properties of bound states of heavy quarks (quarkonia) in an anisotropic plasma.

In quantum chromodynamics with small t' Hooft coupling at short distances nonrelativistic quarkonium states exist. Their binding energies are much smaller than the quark mass $m_Q \gg \Lambda_{\rm QCD}$ ($Q = c, b$), and their size is much larger than $1/m_Q$. At zero temperature, since the velocity of the quarks in the bound state is small, $v \ll 1$, quarkonium can be understood in terms of nonrelativistic potential models [1] using the Cornell potential [2]. The potential model can actually be derived directly from QCD as an effective field theory (potential nonrelativistic QCD - pNRQCD) by integrating out modes above the scales m_Q and then $m_Q v$, respectively [3].

At high temperatures, the deconfined phase of QCD exhibits screening of static color-electric fields [4]. It is expected that this screening leads to the dissociation of quarkonium states, which can serve as a signal for the formation of a deconfined quark-gluon plasma in heavy-ion collisions [5]. Inspired by the success at zero temperature, potential model descriptions have also been applied to understand quarkonium properties at finite temperature. The pioneering paper of Matsui and Satz [5] was followed by the work of Karsch, Mehr and Satz (KMS) [6], which presented the first quantitative calculation. In recent works more involved calculations of quarkonium spectral functions and meson current correlators obtained from potential models have been performed [7–12]. The results have been compared to first-principle QCD calculations performed numerically on lattices [13–16]. A summary and review of the current understanding of these potential models is presented in [17], and different aspects of quarkonium in collider experiments can be found in [18]. More recently the imaginary part of the potential due to Landau damping has been calculated [19,20]. Also, the derivation of potential models from QCD via effective field theory methods has been extended to finite T [21]. All of these works, however, have been performed with the assumption of an isotropic thermal medium.

Here, we attempt a first assessment of the properties of quarkonium states in a QCD plasma which exhibits an anisotropy in momentum space. Such anisotropy may arise due to a locally anisotropic hydrodynamic expansion of a plasma with nonvanishing shear viscosity. It leads to an angular dependence of the $Q\overline{Q}$ potential [22]. We note that the nonequilibrium effect described here arises beyond the linear response approximation in that the operators corresponding to various properties of quarkonium states need to be evaluated in an ensemble of anisotropic (in momentum space) gauge field configurations.

After reviewing the anisotropic plasma in Sec. II, we formulate the first potential model for an anisotropic medium in Sec. III. The solution of the three-dimensional Schrödinger equation is described in Sec. IV, and the numerical results are presented in Sec. 9. We note that by now it is understood that merely solving the Schrödinger

equation for the individual states is not enough, especially close to the continuum threshold. Here many-body interactions should be taken into consideration by solving the Schrödinger equation for the nonrelativistic Green's function [12]. However, for the purpose of the present work the simple analysis suffices. We summarize our results and draw our conclusions in Sec. VI.

THE ANISOTROPIC PLASMA

The phase-space distribution of gluons is assumed to be given by the following *ansatz* [22–26]:

$$f(\mathbf{p}) = f_{\rm iso}(\sqrt{\mathbf{p}^2 + \xi(\mathbf{p}\cdot\mathbf{n})^2}). \quad (1)$$

Thus, $f(\mathbf{p})$ is obtained from an isotropic distribution $f_{\rm iso}(|\mathbf{p}|)$ by removing particles with a large momentum component along $\mathbf{n}$, the direction of anisotropy. We shall restrict ourselves here to a plasma close to equilibrium, which is motivated by the fact that in a heavy-ion collision quarkonium states are expected to form when the temperature has dropped to (1-2) T_c; by then, the plasma may have equilibrated at least partly. Hence, we assume that the function $f_{\rm iso}(|\mathbf{p}|)$ is a thermal ideal-gas distribution.

The parameter ξ determines the degree of anisotropy,

$$\xi = \frac{1}{2}\frac{\langle \mathbf{p}_\perp^2 \rangle}{\langle p_z^2 \rangle} - 1, \quad (2)$$

where $p_z \equiv \mathbf{p}\cdot\mathbf{n}$ and $\mathbf{p}_\perp \equiv \mathbf{p} - \mathbf{n}(\mathbf{p}\cdot\mathbf{n})$ denote the particle momentum along and perpendicular to the direction $\mathbf{n}$ of anisotropy, respectively. If ξ is small then it is also related to the shear viscosity of the plasma; for example, for one-dimensional boost-invariant expansion [27]

$$\xi = \frac{10}{T\tau}\frac{\eta}{s}, \quad (3)$$

where T is the temperature, τ is proper time (and $1/\tau$ is the Hubble expansion rate), and η/s is the ratio of shear viscosity to entropy density. In an expanding system, nonvanishing viscosity (finite momentum relaxation rate) implies an anisotropy of the particle momenta which increases with the expansion rate $1/\tau$. For $\eta/s \simeq 0.1$ – 0.2 and $\tau T \simeq 1$ – 3 one finds that $\xi \simeq 1$.

We should stress that in this paper we restrict to solving the time-independent Schrödinger equation, i.e. we assume that the plasma is at a constant temperature T and anisotropy ξ. This approximation is useful if the time scale associated with the bound state, $\sim 1/|E_{\rm bind}|$, is short compared to the time scales over which T and ξ vary. Indeed, for sufficiently large quark mass m_Q this condition should be satisfied.

THE KARSCH-MEHR-SATZ MODEL AT FINITE TEMPERATURE

Isotropic medium ($\xi = 0$)

Lacking knowledge of the exact heavy-quark potential at finite temperature, different phenomenological potentials, as well as lattice-QCD based potentials have been used in potential models to study quarkonium.

The KMS model [6] assumes the following form of the heavy-quark potential at finite temperature in an isotropic plasma with $\xi = 0$:

$$F(r,T) = -\frac{\alpha}{r}\exp(-m_D r) + \frac{\sigma}{m_D}[1 - \exp(-m_D r)]. \quad (4)$$

Here, $\alpha \approx 0.385$ is an effective Coulomb coupling at (moderately) short distances, $\sigma = 0.223$ GeV2 is the string tension and $m_D(T)$ is the Debye screening mass.

Equation (4) is a model for the action of a Wilson loop of size $1/T$ and r in the temporal and spatial directions, respectively, (see [28] and references therein). This potential has been used before to study quarkonium bound states [7]. However, it was realized shortly after that Eq. (4) cannot be taken directly as the heavy-quark potential because it contains an entropy contribution; see, for example, the discussion in Refs. [12,17,28,29]. Rather, Eq. (4) corresponds to the free energy due to the presence of a $Q\overline{Q}$ in the medium. We emphasize that the entropy term in the *lattice data* is merely a perturbative entropy contribution present at large distances[1], $r \to \infty$, and it is absent at short distances [28]. One can remove this entropy term from the lattice data by parametrizing $F(r \to \infty, T) \equiv F_\infty(T)$ in the form $F_\infty(T) = a/T - bT$ and then adding the term bT to $F(r,T)$ at large distance, thereby obtaining what has been called *the physical potential* in [11,12].

Alternatively, one could calculate the full entropy $S = -\partial F/\partial T$ and add it to the free energy, which leads to the internal energy $U = F + TS$. The internal energy calculated in lattice QCD [30] shows a large increase in U_∞ near T_c, due to the large increase of the entropy near T_c. Furthermore, at temperatures $T \simeq T_c$ a potential model based on the internal energy becomes much more binding than the $T = 0$ Cornell potential (we refer to this as "overshooting"). For these reasons, the internal energy $U(r,T)$ obtained on the lattice should neither be identified with the heavy-quark potential, although it has been used in potential models before [7,10,29]. Nevertheless, the internal energy provides a useful upper limit for the potential at finite T. A version of the internal energy in which the overshooting problem was eliminated, was designed in [11,12] and called the *most confining potential*.

In this paper we also construct a model for a potential which could be viewed as an upper limit for the heavy-quark potential, i.e. $V_\infty \simeq U_\infty$. Our present model is very

[1]We evaluate it in anisotropic HTL resummed perturbation theory in Sec. 3.

simple and contains a minimum number of parameters, as the primary goal is to generalize the finite-T potential to anisotropic media. In our model we add the full entropy contribution to the KMS *ansatz* (4):

$$V(r,T) = F(r,T) - T\frac{\partial F(r,T)}{\partial T} \tag{5}$$

$$\approx -\frac{\alpha}{r}(1+m_D r)\exp(-m_D r) + 2\frac{\sigma}{m_D}[1-\exp(-m_D r)] - \sigma r \exp(-m_D r). \tag{6}$$

In the second line we have used that m_D is approximately proportional to T at high temperatures. Since the effect of the running of the coupling is important only at distances <0.1 fm, not relevant for quarkonium studies, here we do not consider running-coupling corrections. Figure 1 compares the potential at finite temperature to that at $m_D = 0$ which is a Cornell potential.

This potential, just as its original form (4), essentially represents an interpolation from the well-known Cornell potential at short distance to an exponentially Debye-screened string attraction at large r. With $g \simeq 2$, $m_D \simeq gT$ and $T_c \simeq 200$ MeV, the length scale where medium effects become large is roughly given by $r_{\rm med}(T) \simeq T_c/(2T)$ fm, in approximate agreement with lattice results from Ref. [31]. In (6) corrections to the Cornell potential are suppressed at distances $r < 1/m_D$, i.e. they appear only at order $(m_D r)^2$. This is due to the fact that we subtracted the derivative $\partial F/\partial \log T$ even at intermediate distances; it appears to give a better representation of the lattice potential at $r < r_{\rm med}(T)$, which in fact coincides with the Cornell *ansatz*. One can see in Fig. 1 that our potential $V(r)$ is very close to the Cornell potential for distances up to $r \simeq 0.4$ fm, in agreement with lattice results [31]. The finite-temperature potential (6) does not overshoot the Cornell potential significantly at any r [11], at least up to temperatures on the order of $1.5T_c$. This is actually the temperature range where most bound states (except perhaps 1S bottomonium) are expected to dissociate in an isotropic medium [11,12]. On the other hand, Fig. 1 shows that at rather high temperatures of order $3T_c$, the model (6) *does* overshoot the Cornell potential at short distances. This indicates that this simple form of the finite-T potential is not appropriate when the Debye mass m_D is large. However, this regime is not of interest here since even the $b\bar{b}$ states are no longer bound. Overall, the potential (6) appears to provide a reasonable model for the interquark potential in the deconfined phase at (moderately) high temperatures.

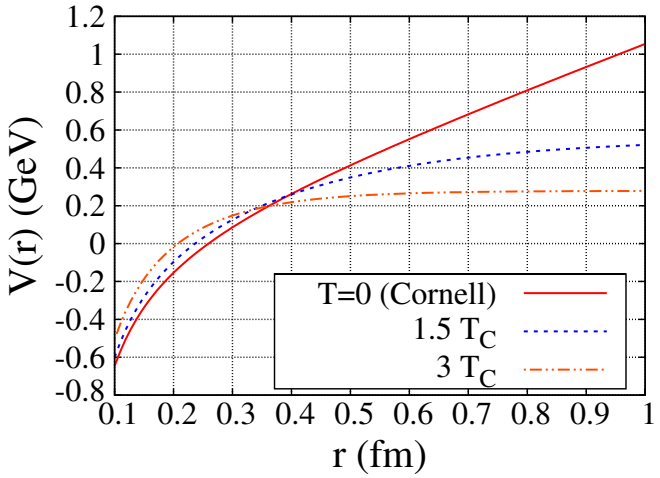

FIG. 1 (color online). The model potential from Eq. (6) at zero and at finite temperature as a function of distance. Temperature is normalized to $T_c = 192$ MeV and the temperature dependence of the Debye mass is parametrized as given in Eq. (31) below.

At $r \to \infty$ the potential (6) approaches

$$V_\infty(T) = 2\frac{\sigma}{m_D} \simeq \frac{0.16\text{GeV}^2}{T}. \tag{7}$$

Again, this is in approximate agreement with the $V_\infty \simeq 1/T$ ansatz used in Ref. [11]. Note, in particular, that (7) is about the same as the internal energy $U_\infty(T)$ obtained from the lattice data [11]. We take this as an indication that our potential (6) represents an upper limit for the possible finite-temperature potentials.

The main assumption of the KMS model is that the very same screening scale m_D which emerges in the Debye-Coulomb potential also appears in the nonperturbative, long-distance contribution due to the string. In the following, we take over this assumption to anisotropic plasmas.

It is interesting to note that the KMS *ansatz* for the free energy from Eq. (4) can be obtained in the usual way from the Fourier transform of the static propagator, provided that a nonperturbative contribution

$$\frac{m_G^2}{(\mathbf{k}^2 + m_D^2)^2} \tag{8}$$

is added to the standard HTL resummed propagator [32]. Here, m_G^2 is a constant of dimension two which can be related to the string tension σ by matching onto a Cornell potential at small $m_D r$. The presence of such an additional dimensionful scale (besides T) also leads to a nonvanishing trace of the energy-momentum tensor [33].

Anisotropic medium ($\xi > 0$)

Our fundamental assumption is that the modified KMS potential (6), which provides a reasonable upper-limit model for the heavy-quark potential in isotropic media, retains its basic form also when the local momentum distribution of the plasma particles is anisotropic ($\xi > 0$). However, the isotropic Debye mass $m_D(T)$ is now replaced by an angular dependent screening scale $\mu(\theta;\xi,T)$ as discussed in the next section.

Angular dependence of the potential at short distances

The potential from one-gluon exchange at short distance can be evaluated perturbatively. At tree level the potential corresponds to the Fourier transform of the static gluon propagator which resums screening effects at high temperature[2]. For $\xi > 0$ the potential depends not only on the distance between the Q and $\overline{Q}$ but also on the angle θ between their separation $\mathbf{r}$ and the direction $\mathbf{n}$ of anisotropy [22].

To linear order in ξ, the potential can be expressed as

$$V(\mathbf{r}, \xi) = V_{\rm iso}(r) - g^2 C_F \xi m_D^2 \int \frac{d^3\mathbf{p}}{(2\pi)^3} e^{i\mathbf{p}\cdot\mathbf{r}} \frac{\frac{2}{3} - (\mathbf{p}\cdot\mathbf{n})^2/\mathbf{p}^2}{(\mathbf{p}^2 + m_D^2)^2} \quad (9)$$

$$= V_{\rm iso}(r)(1 - \xi \mathcal{F}(\hat{r}, \theta)), \quad (10)$$

where $\hat{r} \equiv r m_D$ and $m_D(T)$ denotes the screening mass in the isotropic medium at a given temperature T, as before. Also, $V_{\rm iso}(r)$ is the Debye-screened Coulomb potential in an isotropic medium, as given by the first term in Eq. (4), and the function

$$\mathcal{F}(\hat{r}, \theta) \equiv f_0(\hat{r}) + f_1(\hat{r}) \cos(2\theta) \quad (11)$$

with

$$f_0(\hat{r}) = \frac{6(1 - e^{\hat{r}}) + \hat{r}[6 - \hat{r}(\hat{r} - 3)]}{12\hat{r}^2} = -\frac{\hat{r}}{6} - \frac{\hat{r}^2}{48} + \cdots, \quad (12)$$

$$f_1(\hat{r}) = \frac{6(1 - e^{\hat{r}}) + \hat{r}[6 + \hat{r}(\hat{r} + 3)]}{4\hat{r}^2} = -\frac{\hat{r}^2}{16} + \cdots. \quad (13)$$

Note that Eqs. (9)-(13) do not apply at large distances $\hat{r} \gg 1$, which is a shortcoming of the Taylor expansion of the full potential in powers of ξ. This is of no importance in the following because these expressions are used at short distances only in order to determine the angular dependence of the screening scale, which will then replace m_D in Eq. (6).

We can now define the θ-dependent screening mass in the anisotropic medium as the inverse of the distance scale $r_{\rm med}(\theta)$ over which $|rV(r)|$ drops by a factor of e:

$$\log \frac{-\alpha}{r_{\rm med} V(r_{\rm med}, \theta; \xi, T)} = 1, \quad (14)$$

$$\mu(\theta; \xi, T) = r_{\rm med}^{-1}(\theta; \xi, T). \quad (15)$$

[2]In the first part of this section we are only interested in distances up to $\sim 1/\mu$. It is therefore not crucial to distinguish carefully whether the potential is identified with the Fourier transform of the propagator or with the internal energy. We shall add the entropy contribution later, c.f. Eqs. (18)-(19), to suppress corrections to the Cornell potential at short distances.

In (14) we have used the fact that $rV \to -\alpha$ as $r \to 0$. To leading order in ξ this leads to

$$\hat{r}_{\rm med} = 1 - \xi \mathcal{F}(\hat{r}_{\rm med}, \theta). \quad (16)$$

An approximate solution to Eq. (16) is given by

$$\hat{r}_{\rm med} \simeq 1 + \xi \frac{3 + \cos 2\theta}{16} \Rightarrow \frac{\mu}{m_D} \simeq 1 - \xi \frac{3 + \cos 2\theta}{16}. \quad (17)$$

For $\xi = 0.5$ (1.0) this solution achieves a relative accuracy of $\leq 4\%$ ($\leq 18\%$) over the entire range of θ. The accuracy of this result can be improved systematically by going beyond $\mathcal{O}(\hat{r}^2)$ in the expansion of the functions f_0 and f_1 introduced in Eqs. (12),(13).

The "minimal" extension of the KMS model to nonzero anisotropy consists of replacing $m_D(T)$ in (6) by $\mu(\theta; \xi, T)$ from above:

$$V(\mathbf{r}) = -\frac{\alpha}{r}(1 + \mu r)\exp(-\mu r) + \frac{2\sigma}{\mu}[1 - \exp(-\mu r)] - \sigma r \exp(-\mu r). \quad (18)$$

At short distances this reduces to the Cornell potential $V(r) = -\alpha/r + \sigma r$, as it should be.

Corrections to Eq. (18) due to the finite quark mass can be accounted for by adding a temperature- and spin-independent correction proportional to $\sigma/(m_Q^2 r)$ [34]. This improves the accuracy of the wave functions of quarkonium states obtained from the solution of the nonrelativistic Schrödinger equation. The potential finally takes the form

$$V(\mathbf{r}) = -\frac{\alpha}{r}(1 + \mu r)\exp(-\mu r) + \frac{2\sigma}{\mu}[1 - \exp(-\mu r)] - \sigma r \exp(-\mu r) - \frac{0.8\sigma}{m_Q^2 r}. \quad (19)$$

Perturbative heavy-quark free energy in an anisotropic medium

In the limit of infinite mass, the free energy of a heavy quark in a thermal plasma is related to the expectation value of Polyakov loops. At high temperature, this can be calculated within hard-thermal loop resummed perturbation theory. The leading-order contribution is given by

$$F_Q(\xi, T) = -\frac{1}{2}(ig)^2 C_F \int \frac{d^3k}{(2\pi)^3}[\Delta^{00}(\mathbf{k}) - \frac{1}{\mathbf{k}^2}], \quad (20)$$

where $\Delta^{00}(\mathbf{k})$ is the "hard thermal loop" resummed propagator of static A_0 fields. We have subtracted the temperature-independent contribution to F_Q which is not of interest here. Also, this renders the integral UV-finite. For the case of an anisotropic medium, $\Delta^{00}(\mathbf{k})$ has been calculated in Ref. [22]; see, also, Ref. [35]. The expression (20) then turns into

$$F_Q(\xi, T) = -\frac{1}{2}\alpha_s C_F m_D h(\xi), \tag{21}$$

with a temperature-independent function $h(\xi)$. For small anisotropy the following expansion in ξ applies:

$$h(\xi) = 1 - \frac{1}{6}\xi + \frac{18 - \pi^2}{240}\xi^2 + \cdots \tag{22}$$

We identify this expression with the free energy of a quark due to its interaction with the medium (i.e., half the free energy of a $Q\overline{Q}$ pair at large separation). However, the perturbative entropy contribution $TS = -T\partial F_Q/\partial T$ should be added again in order to obtain the potential. Since (21) is linear in T (at fixed coupling), it follows that the perturbative contribution to V_∞ vanishes[3]. On the other hand, lattice data (for an isotropic medium) indicate that the free energy of a quark-antiquark pair at infinite separation also contains a nonperturbative contribution of the form $V_\infty(T) = r_{\rm med}(T)\sigma$ [12], which agrees qualitatively with the prediction of the KMS model, $V_\infty \sim \sigma/m_D$. Within the framework of the KMS model, this implies that at $\xi \neq 0$, $V_\infty(\theta; \xi, T)$ depends on angle as screening becomes anisotropic.

SOLVING THE 3D SCHRÖDINGER EQUATION

To determine the wave functions of bound quarkonium states, we solve the Schrödinger equation

$$\hat{H}\phi_\upsilon(\mathbf{x}) = E_\upsilon\phi_\upsilon(\mathbf{x}), \hat{H} = -\frac{\nabla^2}{2m_R} + V(\mathbf{x}) + m_1 + m_2, \tag{23}$$

on a three-dimensional lattice in coordinate space with the potential given in Eq. (19). Here m_1 and m_2 are the masses of the two heavy quarks and m_R is the reduced mass: $m_R = m_1 m_2/(m_1 + m_2)$. The index υ on the eigenfunctions, ϕ_υ, and energies, E_υ, represents a list of all relevant quantum numbers, e.g. n, l, and m for a radial Coloumb potential. Because of the anisotropic screening scale, the wave functions are no longer radially symmetric if $\xi \neq 0$. Since we consider only small anisotropies we nevertheless label the states as $1S$ (ground state) and $1P$ (first excited state), respectively.

To find solutions to Eq. (23) we use the finite difference time domain method (FDTD) [36]. In this method we start with the time-dependent Schrödinger equation

$$i\frac{\partial}{\partial t}\psi(\mathbf{x}, t) = \hat{H}\psi(\mathbf{x}, t), \tag{24}$$

which can be solved by expanding in terms of the eigenfunctions, ϕ_υ:

$$\psi(\mathbf{x}, t) = \sum_\upsilon c_\upsilon\phi_\upsilon(\mathbf{x})e^{-iE_\upsilon t}. \tag{25}$$

If one is only interested in the lowest energy states (ground state and first few excited states) an efficient way to proceed is to transform (24) and (25) to Euclidean time by a Wick rotation, $\tau \equiv it$:

$$\frac{\partial}{\partial\tau}\psi(\mathbf{x}, \tau) = -\hat{H}\psi(\mathbf{x}, \tau), \tag{26}$$

and

$$\psi(\mathbf{x}, \tau) = \sum_\upsilon c_\upsilon\phi_\upsilon(\mathbf{x})e^{-E_\upsilon\tau}. \tag{27}$$

For details of the algorithm we refer to Ref. [36].

Finding the ground state

By definition the ground state is the state with the lowest energy eigenvalue, E_0. Therefore, at late imaginary time the sum over eigenfunctions (27) is dominated by the ground state eigenfunction

$$\lim_{\tau\to\infty}\psi(\mathbf{x}, \tau) \to c_0\phi_0(\mathbf{x})e^{-E_0\tau}. \tag{28}$$

Because of this one can obtain the ground state wave function, ϕ_0, and energy, E_0, by solving Eq. (26) starting from a random three-dimensional wave function, $\psi_{\rm initial}(\mathbf{x}, 0)$, and evolving forward in imaginary time. This initial wave function should have nonzero overlap with all eigenfunctions of the Hamiltonian; however, due to the damping of higher-energy eigenfunctions at sufficiently late imaginary times we are left with only the ground state, $\phi_0(\mathbf{x})$. Once the ground state wave function (or, in fact, any other wave function) is found we can compute its energy eigenvalue via

$$E_\upsilon(\tau \to \infty) = \frac{\langle\phi_\upsilon|\hat{H}|\phi_\upsilon\rangle}{\langle\phi_\upsilon|\phi_\upsilon\rangle} = \frac{\int d^3\mathbf{x}\phi_\upsilon^*\hat{H}\phi_\upsilon}{\int d^3\mathbf{x}\phi_\upsilon^*\phi_\upsilon}. \tag{29}$$

To obtain the binding energy of a state, $E_{\upsilon,\rm bind}$, we subtract the quark masses and the potential at infinity

$$E_{\upsilon,\rm bind} \equiv E_\upsilon - m_1 - m_2 - \frac{\langle\phi_\upsilon|V(\theta, |\mathbf{r}| \to \infty)|\phi_\upsilon\rangle}{\langle\phi_\upsilon|\phi_\upsilon\rangle}. \tag{30}$$

For the isotropic KMS potential the last term is independent of the quantum numbers υ and equal to σ/m_D. In the anisotropic case, however, this is no longer true since the operator $V_\infty(\theta)$ carries angular dependence, as already discussed above. Its expectation value is of course independent of θ but does depend on the anisotropy parameter ξ.

Finding the excited states

The basic method for finding excited states is to first evolve the initially random wave function to large imagi-

[3]A term $F_Q \sim a/T$ could be generated by a nonperturbative contribution of the form $m_G^2/(\mathbf{k}^2 + m_D^2)^2$ to the static gluon propagator, as already mentioned above. m_G^2 is a constant of dimension two [32].

nary times, find the ground state wave function, ϕ_0, and then project this state out from the initial wave function and reevolve the partial-differential equation in imaginary time. However, there are (at least) two more efficient ways to accomplish this. The first is to record snapshots of the three-dimensional wave function at a specified interval $\tau_{\rm snapshot}$ during a single evolution in τ. After having obtained the ground state wave function, one can then go back and extract the excited states by projecting out the ground state wave function from the recorded snapshots of $\psi(\mathbf{x}, \tau)$.

An alternative way to select different excited states is to impose a symmetry condition on the initially random wave function which cannot be broken by the Hamiltonian evolution. For example, one can select the first excited state of the (anisotropic) potential by antisymmetrizing the initial wave function around either the x, y, or z axes. In the anisotropic case this trick can be used to separate the different polarizations of the first excited state of the quarkonium system and to determine their energy eigenvalues with high precision. This high precision allows one to more accurately determine the splitting between polarization states which are otherwise degenerate in the isotropic Debye-Coulomb potential.

Whichever method is used, once the wave function of an excited state has been determined one can again use the general formulas (29) and (30) to determine its binding energy.

RESULTS AND DISCUSSION

In this section we present the solutions of the three-dimensional Schrödinger Eq. (23) in a weakly anisotropic medium. In particular, we determine the temperature dependence of the binding energies of different charmonium and bottomonium states obtained with the anisotropic potential (19) that has been constructed from the *most binding* isotropic potential. The anisotropy- and temperature-dependent screening mass $\mu(\theta; \xi, T)$ is given in Eq. (17). To illustrate the effect of the anisotropy of the medium more clearly we shall also compare the results to those obtained for an isotropic medium. In the latter case $\xi = 0$ and so $\mu(\theta; \xi, T) = m_D(T)$, where the temperature dependence of the Debye mass is given by

$$m_D(T) = AgT\sqrt{(1 + n_f/6)}. \tag{31}$$

For $n_f = 2$ number of massless quark flavors the parameter $A = 1.4$ has been determined in lattice calculations [37]. We choose a fixed gauge coupling of $g = 1.72$ which yields $m_D(T)/T \approx 2.8$. This agrees approximately with lattice estimates of m_D/T for temperatures on the order of $T/T_c \sim 1.5$, and it also gives a reasonable estimate of the free energy at infinite separation [37]. The values of the charm and bottom quark masses are chosen such that at low temperature the correct masses of $M_{J/\psi} = 3.1$ GeV and $M_\Upsilon = 9.4$ GeV for the J/ψ and the Υ, respectively, are recovered. Accordingly,

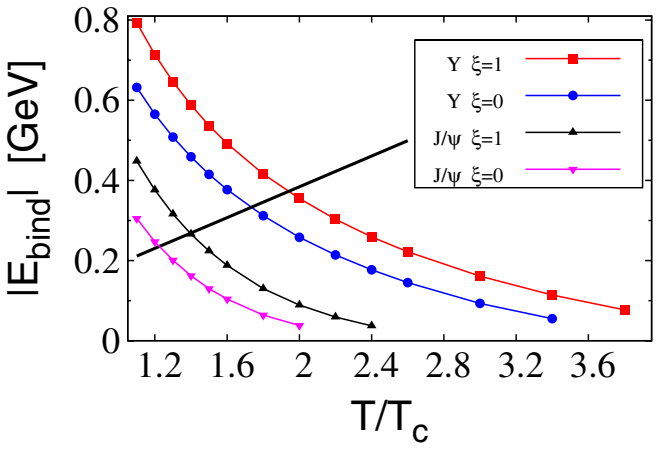

FIG. 2 (color online). Temperature-dependence of the binding energies $|E_{\rm bind}|$ for the ground states of charmonium (lower curves) and bottomonium (upper curves) in the vector channel for two values of the plasma anisotropy parameter ξ. The straight line corresponds to a binding energy equal to the temperature.

$$m_c = 1.3\text{GeV} \quad \text{and} \quad m_b = 4.7\text{GeV}. \tag{32}$$

All of the results reported below were obtained from lattices with lattice spacings approximately 20 times smaller than the root-mean-square radius $\langle \mathbf{r}^2 \rangle_\upsilon^{1/2} \times (T, \xi, m_Q)$ of the state under consideration, defined by the quantum number υ. The lattice size L was chosen to be about 6 times larger than the RMS radius[4]. Discretization errors and finite-size effects are thus expected to be reasonably small and nearly independent of T, ξ, m_Q, and υ. We stopped the time evolution when the energy $E_\upsilon(\tau)$ of the state had stabilized to within 10^{-8}. A more detailed investigation of numerical errors is beyond the scope of the present paper. Our goal here is to show how quarkonium states may be affected by the anisotropy of the medium.

The temperature dependence of the binding energies of charmonium and bottomonium ground states in the vector channel[5] are depicted in Fig. 2. The figure shows the results obtained for isotropic $\xi = 0$ and anisotropic $\xi = 1$ media. The former are in agreement with those obtained in Ref. [11] with the so-called *most-confining* isotropic potential. As expected, the binding energy decreases as the screening mass $m_D(T)$ increases with temperature T. This plot also indicates that $|E_{\rm bind}|$ increases with the anisotropy

[4]Since we restrict the analysis to only weak medium anisotropies, we employ isotropic lattices with uniform lattice spacing in all three Cartesian directions.

[5]Spin effects are neglected in our treatment and the ground state could be identified with either the pseudoscalar or the vector state. For definiteness, we shall refer to the vector channel.

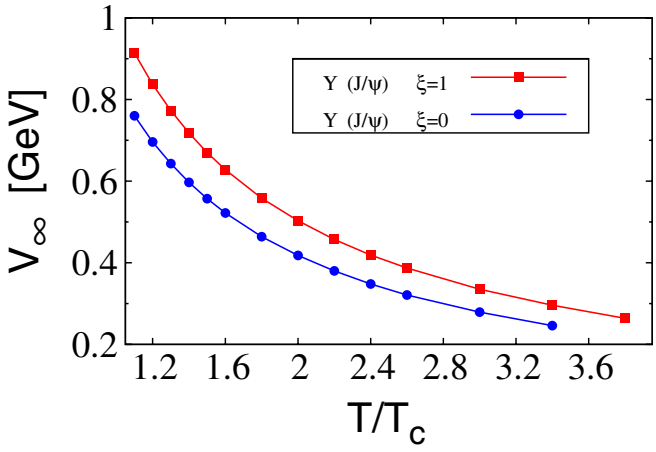

FIG. 3 (color online). Expectation value of V_∞ in the J/Ψ or Υ states as a function of temperature for two values of the plasma anisotropy parameter ξ.

ξ. This can be understood from the fact that in an anisotropic plasma the screening scale $\mu(\theta)$ at a given temperature is smaller than the corresponding Debye mass m_D; see Eq. (17). As a consequence, the screening of the attractive Coulomb and string contributions is less accentuated in the anisotropic plasma and so quarkonium states are bound more strongly than in an isotropic medium. The magnitude of this effect is substantial even for the moderate anisotropy considered here. Near the critical temperature T_c, for example, the binding energy of the 1S vector $c\bar{c}$ ground state increases by about 50%, and that of the 1S $b\bar{b}$ ground state increases by roughly 30% compared to the binding energies calculated in an isotropic medium (the only case addressed previously in the literature).

It is important to highlight another aspect of the reduced screening. In the KMS model the asymptotic value of the potential is intrinsically related to the screening mass via the relation $\langle V_\infty\rangle(T) = \langle v|\sigma\mu^{-1}(\theta;\xi,T)|v\rangle$. This implies that in the anisotropic medium less screening translates into an increase of the potential at infinite separation, V_∞. The above is illustrated in Fig. 3 which shows the expectation value of V_∞ in the Υ state[6]. V_∞, in turn, determines the continuum threshold, which, at a given T is at higher energy than in the isotropic case. This implies that at a given temperature the energy gap between the bound state and the continuum, which is the binding energy, is increased compared to the isotropic case.

Comparing the behavior of $\langle V_\infty\rangle$ to that of the binding energy of the Υ from Fig. 2 shows that the decrease of $|E_{\rm bind}|$ with T is largely due to the decrease of the continuum threshold $\langle V_\infty\rangle$. Indeed, we have confirmed that the wave function of the $b\bar{b}$ ground state is essentially unaffected by the medium, i.e. it is almost independent of T (for $T \lesssim 2T_c$) and ξ (for $\xi \lesssim 1$). This has interesting implications for phenomenology: On one hand, the center of the Υ-peak in the dilepton invariant mass distribution may not shift much (since $V_\infty = 0$ for decay into dileptons) even for temperatures $>T_c$ where the binding energy is significantly lower than in vacuum. On the other hand, when $|E_{\rm bind}| \sim T$ we expect substantial broadening of the states due to direct thermal activation [11,38]. The thermal width can be estimated from the binding energy [38]. When the width is larger than the binding energy, a state decays faster than it binds [11]. Note, that in the same temperature domain collisions with thermal particles of the medium would further broaden the width of a state. Thus, the dissociation of the bound states may be expected to occur roughly when $|E_{\rm bind}| \sim T$ [17]. With the potential investigated in this paper, which likely represents an upper limit for the attractive interaction, the condition $|E_{\rm bind}| \sim T$ is met for the J/ψ by $1.2T_c$ for $\xi = 0$, in agreement with previous results [11], and by $1.4T_c$ for $\xi = 1$. We stress furthermore that the thermal density of a given state,

$$\rho \sim \exp(-\frac{E_{\rm bind}}{T}), \tag{33}$$

is not enhanced significantly when $|E_{\rm bind}| < T$. In other words, since T decreases with time in a heavy-ion collision, quarkonium states with quantum numbers υ should appear at a temperature $T_\upsilon \sim |E_{\upsilon,\rm bind}|$ [7]. From Fig. 2 it is plausible that in a viscous plasma quarkonium synthesis occurs at higher temperature than in a perfectly equilibrated medium. For the J/Ψ for example, $\Delta T_{\rm synth}/T_c \simeq 20\%$ for $\xi = 1$ as compared to $\xi = 0$.

In Fig. 4 we show the root-mean-square (RMS) radii $\langle \mathbf{r}^2\rangle^{1/2}(T,\xi)$ of the $c\bar{c}$ and $b\bar{b}$ ground states as functions of temperature. The former grows rather rapidly about the dissociation point where $|E_{\rm bind}| \sim T$. The size of the Υ, on the other hand, increases only little with temperature. We can understand these results, qualitatively, as follows. For charmonium the string part of the potential dominates, and the growth of its RMS radius with T indicates that screening of the string is strong[8]. We observe a similar behavior of the first $1P$ excited state of bottomonium. On the other hand, $1S$ bottomonium is too small to be affected strongly by screening (for $T \lesssim 2T_c$), it is essentially a Coulomb state. The weaker binding as compared to low temperature is largely due to a decrease of the continuum threshold V_∞, as already mentioned above.

[6]We recall that V_∞ is proportional to the identity at $\xi = 0$ and hence its expectation value is the same for all states. At $\xi = 1$ we obtain a very small difference between $\langle J/\Psi|V_\infty|J/\Psi\rangle$ and $\langle\Upsilon|V_\infty|\Upsilon\rangle$.

[7]The total number of formed quarkonium states depends on how many heavy quarks are produced in the initial hard processes, and on what fraction thereof is bound in D- and B-mesons, respectively.

[8]Recall that the in the KMS model the string tension enters with a factor of $1/m_D(T)$ at intermediate distances on the order of $r \sim 1/m_D(T)$.

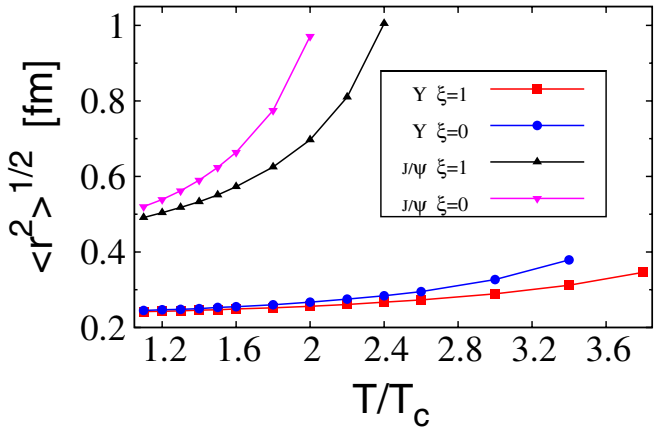

FIG. 4 (color online). Root-mean-square radii of the $1S$ ground states of charmonium (upper curves) and bottomonium (lower curves) as functions of temperature for two values of the plasma anisotropy parameter ξ.

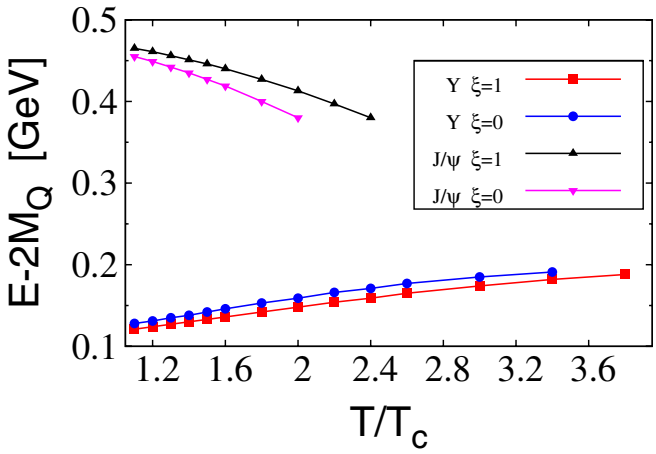

FIG. 5 (color online). Absolute energy of the J/Ψ and Υ states, minus twice the corresponding quark mass, as a function of temperature.

In this vein, it is also instructive to look at the behavior of the absolute energy of the J/Ψ and Υ states versus temperature, shown in Fig. 5. We recall that $E - 2m_Q = \langle V_\infty \rangle + E_{\rm bind}$. The energy of the Υ increases slightly with temperature as is expected for a small-size state bound mainly by the Debye-Coulomb part of the potential (plus a constant): the first term on the right hand side of Eq. (19) *increases* with the screening mass μ. On the other hand, $E_{J/\Psi}$ decreases with T because the second term in (19) *decreases* as μ increases.

Figure 6 shows the temperature dependence of the binding energies of the $1P$ states of bottomonium[9], identified with the χ_b. The anisotropy again leads to an increase of $|E_{\rm bind}|$ by about 50%, comparable to the behavior of the

[9]The $1P$ states of charmonium do not have binding energies which exceed the temperature significantly for $T \gtrsim T_C$.

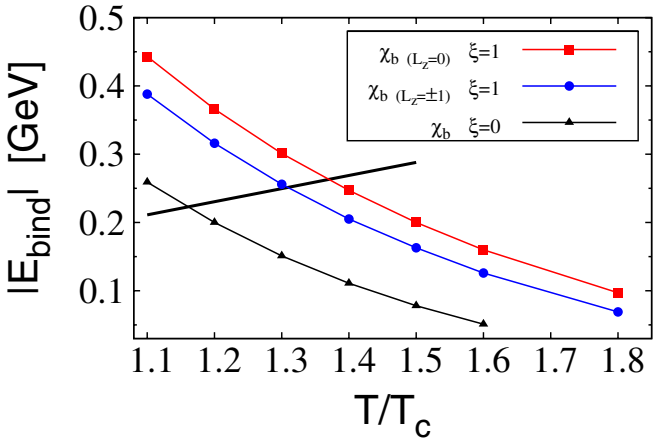

FIG. 6 (color online). Temperature-dependence of the binding energy for the $1P$ state of bottomonium for two values of the plasma anisotropy parameter ξ. The straight line corresponds to a binding energy equal to the temperature.

J/Ψ from above. It also leads to a preferred polarization of the χ_b, with about 50 MeV splitting between states with angular momentum $L_z = 0$ and $L_z = \pm 1$, respectively. At $T \sim T_c$, due to the Boltzmann factor (33), the population of the state with $L_z = 0$ is about 30% higher than that of either one of the $L_z = \pm 1$ states. Here, the polarization is with respect to the axis $\mathbf{n}$ of anisotropy, which coincides with the direction of expansion of the plasma. In addition, quarkonium states produced in high-energy collisions initially through semihard gluon fusion may exhibit polarization with respect to the particle velocity vector [39].

SUMMARY AND CONCLUSIONS

In a viscous plasma, anisotropic expansion of a fluid element leads to an anisotropy of the quasiparticle momentum distributions. The hard thermal loop resummed propagator of static chromo-electric fields then carries angular dependence which leads to anisotropic Debye screening.

In this paper we have proposed the first model for the static potential between a very heavy quark and antiquark in a hot anisotropic QCD plasma. Conceptually, we assume that the time scale $\sim 1/|E_{\rm bind}|$ associated with the bound state is short compared to the time scales over which the temperature and the anisotropy evolve.

At distances on the order of the Debye length the potential can be calculated from perturbative QCD (at high temperature). At larger distances it is however dominated by the non-perturbative string attraction. Lattice gauge theory simulations have shown that in the deconfined phase the string is screened at a similar scale $r_{\rm med}(T) \sim 1/m_D(T)$ and that at infinite separation the free energy of a $Q\bar{Q}$ pair approaches a constant $V_\infty(T)$, equal to twice the free energy of a single heavy quark in the plasma.

The essential features appear to be in qualitative agreement with a model proposed by Karsch, Mehr and Satz [6]

long time ago. However, to obtain the heavy-quark potential we subtract the entropy contribution from their *ansatz* for the free energy of a $Q\bar{Q}$ pair. We thereby obtain the internal energy of the $Q\bar{Q}$ pair which should be viewed as an upper limit for the physical potential. The latter may be less binding than the KMS internal energy used here. We note that in the relevant temperature region, up to about $2T_c$, the potential at short and intermediate distances follows the zero-temperature Cornell-potential; i.e., the overshooting problem of the internal energy is eliminated, in accordance with lattice data on the free energy.

The KMS model correctly reproduces the Cornell potential at short distances and, moreover, does not introduce any new parameters besides the string tension. This is important for our present goal of extending the isotropic potential to anisotropic plasmas. Knowledge of the anisotropic screening scale obtained from the gluon propagator is sufficient to generalize the KMS model to anisotropic media.

We then proceed to solve the Schrödinger equation with this potential to determine the wave functions of bound $c\bar{c}$ and $b\bar{b}$ states in the plasma. The radial Schrödinger equation is no longer sufficient as the potential carries angular dependence. We employ a finite difference time domain method (in Euclidean time) on a three-dimensional lattice to obtain the wave functions and the binding energies. Some medium effects are neglected in this approach. However, solving for the full nonrelativistic Green's function (including threshold effects) in three dimensions is beyond the scope of this paper.

We find that just above the critical temperature $T_c \simeq 192$ MeV for deconfinement (in QCD with $N_c = 3$ colors) in an anisotropic medium both the $1S$ state of charmonium as well as the $1S$ and $1P$ states of bottomonium have binding energies larger than T; the temperature may serve as a rough estimate for the width of the states. The binding energies decrease with temperature and cease to exceed the estimated width $\Gamma \sim T$ at some higher temperatures. We note, also, that the Boltzmann enhancement factor $\exp(-E_{\rm bind}/T)$ for bound states is negligible anyway when $|E_{\rm bind}| \lesssim T$.

The decrease of $|E_{\rm bind}|$ with T is due to two effects: First, the continuum threshold $V_\infty(T)$ decreases approximately like $\sim 1/T$. The energy gap between the bound state and the continuum, which is the binding energy, therefore decreases, too. In fact, for the model adopted here, we find this to be the dominant effect on the $1S$ ground state of bottomonium whose wave function is rather insensitive to the presence of the medium. The state is too small to be affected strongly by screening. Hence, the Υ peak in the dilepton invariant mass distribution may not experience a large shift although one should expect substantial broadening near the dissociation temperature.

Larger states such as the $1S$ ground state of charmonium and the $1P$ excited state of bottomonium, however, may also experience some modifications due to screening. The root-mean-square radii of these states increase rather rapidly with T around the dissociation point $|E_{\rm bind}| \sim T$.

The two main results of this work are as follows. At fixed T, the screening mass decreases with increasing ξ. In the KMS model, the asymptotic value of the potential is intrinsically related to the screening mass via $V_\infty(\theta) \sim 1/\mu(\theta; \xi, T)$. Hence, less screening translates into an increase of the potential at infinite separation. This implies that the binding energies of bound states increase, too. The effect is quite substantial even for moderate anisotropies $\xi \simeq 1$ considered here: we find that just above T_c the binding energy of the bottomonium ground state increases by about 30%, that of $1S$ charmonium and of $1P$ bottomonium by 50%. Thus, such quarkonium states may exist up to somewhat higher temperatures than in case of an isotropic, perfectly equilibrated medium (for $\xi = 0$ the J/ψ and the Υ are expected to dissociate by $1.2T_c$ and $1.8T_c$, respectively, in agreement with previous potential model calculations).

The other important new effect identified here is that the angular dependence of the interquark potential in an anisotropic medium induces a polarization of states with nonzero angular momentum. According to our estimates, the splitting of the χ_b with $L_z = 0$ and $L_z = \pm 1$, respectively, is on the order of 50 MeV. At $T \simeq 200$ MeV, the population of the state with $L_z = 0$ is Boltzmann-enhanced by about 30% as compared to the states with angular momentum along the direction of anisotropy, respectively. The experimental confirmation of such a polarization at RHIC or LHC may provide first evidence for a nonzero viscosity of QCD near T_c.

The next step of our investigation is the determination of the imaginary part of the potential, which will provide insight into how the anisotropy of the medium affects the widths of the states. We shall present results in a future publication.

ACKNOWLEDGMENTS

We thank D. Kharzeev and P. Petreczky for reading the manuscript prior to publication and for useful comments. Y. G. thanks the Helmholtz foundation and the Otto Stern School at Frankfurt university for their support and the center for scientific computing (CSC) for computational resources.

[1] W. Lucha, F. F. Schoberl and D. Gromes, Phys. Rep. **200**, 127 (1991).

[2] E. Eichten, K. Gottfried, T. Kinoshita, J. B. Kogut, K. D. Lane and T. M. Yan, Phys. Rev. Lett. **34**, 369 (1975); **36**, 1276 (1976); E. Eichten, K. Gottfried, T. Kinoshita, K. D. Lane and T. M. Yan, Phys. Rev. D **17**, 3090 (1978); **21**, 313 (1980)**21**, 203 (1980).

[3] A. Pineda and J. Soto, Nucl. Phys. B, Proc. Suppl. **64**, 428 (1998);N. Brambilla, A. Pineda, J. Soto and A. Vairo, Rev. Mod. Phys. **77**, 1423 (2005) .

[4] E. V. Shuryak, Phys. Rep. **61**, 71 (1980);D. J. Gross, R. D. Pisarski and L. G. Yaffe, Rev. Mod. Phys. **53**, 43 (1981).

[5] T. Matsui and H. Satz, Phys. Lett. B **178**, 416 (1986).

[6] F. Karsch, M. T. Mehr and H. Satz, Z. Phys. C **37**, 617 (1988).

[7] Á. Mócsy and P. Petreczky, Phys. Rev. D **73**, 074007 (2006); Eur. Phys. J. C **43**, 77 (2005).

[8] C. Y. Wong, Phys. Rev. C **72**, 034906 (2005).

[9] W. M. Alberico, A. Beraudo, A. De Pace and A. Molinari, Phys. Rev. D **75**, 074009 (2007); Phys. Rev. D **77**, 017502 (2008).

[10] D. Cabrera and R. Rapp, Phys. Rev. D **76**, 114506 (2007).

[11] Á. Mócsy and P. Petreczky, Phys. Rev. Lett. **99**, 211602 (2007).

[12] Á. Mócsy and P. Petreczky, Phys. Rev. D **77**, 014501 (2008).

[13] S. Datta, F. Karsch, P. Petreczky and I. Wetzorke, Phys. Rev. D **69**, 094507 (2004).

[14] A. Jakovác, P. Petreczky, K. Petrov and A. Velytsky, Phys. Rev. D **75**, 014506 (2007).

[15] G. Aarts *et al.*, Phys. Rev. D **76**, 094513 (2007).

[16] T. Umeda, Phys. Rev. D **75**, 094502 (2007).

[17] Á. Mócsy, arXiv:0811.0337

[18] N. Armesto *et al.*, J. Phys. G **35**, 054001 (2008); R. Rapp, D. Blaschke and P. Crochet, arXiv:0807.2470.

[19] M. Laine, O. Philipsen and M. Tassler, J. High Energy Phys. 09 (2007) 066; M. Laine, J. High Energy Phys. 05 (2007) 028.

[20] A. Beraudo, J. P. Blaizot and C. Ratti, Nucl. Phys. **A806**, 312 (2008).

[21] N. Brambilla, J. Ghiglieri, A. Vairo and P. Petreczky, Phys. Rev. D **78**, 014017 (2008);M. A. Escobedo and J. Soto, arXiv:0804.0691 .

[22] A. Dumitru, Y. Guo and M. Strickland, Phys. Lett. B **662**, 37 (2008); Y. Guo, arXiv:0809.3873.

[23] P. Romatschke and M. Strickland, Phys. Rev. D **68**, 036004 (2003).

[24] S. Mrowczynski, A. Rebhan and M. Strickland, Phys. Rev. D **70**, 025004 (2004).

[25] P. Romatschke and M. Strickland, Phys. Rev. D **70**, 116006 (2004).

[26] B. Schenke and M. Strickland, Phys. Rev. D **74**, 065004 (2006).

[27] See Eqs. (6-40) in M. Asakawa, S. A. Bass and B. Müller, Prog. Theor. Phys. **116**, 725 (2006).

[28] P. Petreczky, Eur. Phys. J. C **43**, 51 (2005).

[29] E. V. Shuryak and I. Zahed, Phys. Rev. D **70**, 054507 (2004).

[30] O. Kaczmarek, Proc. Sci., POD07 (2007) 043 [arXiv:0710.0498].

[31] O. Kaczmarek, F. Karsch, F. Zantow and P. Petreczky, Phys. Rev. D **70**, 074505 (2004); **72**, 059903 (2005).

[32] E. Megias, E. Ruiz Arriola and L. L. Salcedo, J. High Energy Phys. 01 (2006) 073; Phys. Rev. D **75**, 105019 (2007).

[33] E. Megias, E. R. Arriola and L. L. Salcedo, arXiv:0903.1060v1.

[34] G. S. Bali, K. Schilling and A. Wachter, Phys. Rev. D **56**, 2566 (1997).

[35] R. Baier and Y. Mehtar-Tani, Phys. Rev. C **78**, 064906 (2008).

[36] I. W. Sudiarta and D. J. W. Geldart, J. Phys. A **40**, 1885 (2007).

[37] O. Kaczmarek and F. Zantow, Phys. Rev. D **71**, 114510 (2005).

[38] D. Kharzeev, L. D. McLerran and H. Satz, Phys. Lett. B **356**, 349 (1995).

[39] B. L. Ioffe and D. E. Kharzeev, Phys. Rev. C **68**, 061902 (2003).